# Full-Counting Many-Particle Dynamics: Nonlocal and Chiral Propagation of Correlations

Yuto Ashida[1] and Masahito Ueda[1,2]
[1]*Department of Physics, University of Tokyo, 7-3-1 Hongo, Bunkyo-ku, Tokyo 113-0033, Japan*
[2]*RIKEN Center for Emergent Matter Science (CEMS), Wako, Saitama 351-0198, Japan*

(Received 18 December 2017; published 4 May 2018)

The ability to measure single quanta allows the complete characterization of small quantum systems known as full-counting statistics. Quantum gas microscopy enables one to observe many-body systems at the single-atom precision. We extend the idea of full-counting statistics to nonequilibrium open many-particle dynamics and apply it to discuss the quench dynamics. By way of illustration, we consider an exactly solvable model to demonstrate the emergence of unique phenomena such as nonlocal and chiral propagation of correlations, leading to a concomitant oscillatory entanglement growth. We find that correlations can propagate beyond the conventional maximal speed, known as the Lieb-Robinson bound, at the cost of probabilistic nature of quantum measurement. These features become most prominent at the real-to-complex spectrum transition point of an underlying parity-time-symmetric effective non-Hermitian Hamiltonian. A possible experimental situation with quantum gas microscopy is discussed.

DOI: 10.1103/PhysRevLett.120.185301

The last two decades have witnessed remarkable developments in the ability to detect individual quanta. In small nanoscale devices such as quantum dots, the exchange of electrons with the reservoir has been detected at the single-electron level [1–4]. Photons emitted from atoms or molecules are now routinely detected individually over a broad range of frequencies [5]. In these systems, complete information about the underlying nonequilibrium dynamics can be obtained from the full-counting statistics [6–9], i.e., statistics of the number of detected signals. While related techniques were applied to Bose gases [10–12] and electron leads [13], developments in this direction have been made for quantum objects with relatively small degrees of freedom.

Meanwhile, recent advances in quantum gas microscopy [14–23] have enabled one to detect atoms trapped in an optical lattice at the single-atom precision. Already, a number of groundbreaking experiments, such as direct observations [24–26] of light-cone spreading of correlations limited by the Lieb-Robinson (LR) velocity $v_{\mathrm{LR}}$ [27–29], and measurements of entanglement entropy [30] and antiferromagnetic correlations [31–34], have been achieved. Similar techniques are available in trapped ions [35,36]. On another front, various types of controlled dissipation have been realized in quantum gases [37–44]. These developments suggest the possibilities of measuring *open many-body* systems at the single-quantum level.

The aim of this Letter is to extend the idea of full-counting statistics to nonequilibrium many-particle dynamics. We consider a many-particle system coupled to a Markovian reservoir. We discuss the full-counting dynamics that give the time evolution of the density matrix conditioned on the number of quantum jumps. A quantum jump refers to a discrete stochastic event due to the action of a jump operator known as the Lindblad operator $\hat{L}_a$ [45]. Physically, this operator describes the detection of a specific measurable signal. Depending on each realization of quantum jumps, the system evolves in time stochastically along what is referred to as trajectory. Trajectories can then be classified according to the number of jumps. We find nonlocal and chiral propagation of correlations and a concomitant oscillatory entanglement growth. These features originate from the non-Hermiticity of the underlying open quantum dynamics and become most prominent at the spectrum transition point of the parity-time ($PT$) symmetric Hamiltonian [46]. We also discuss a possible experimental realization by quantum gas microscopy.

From a broader perspective, previous studies on open quantum dynamics have revealed emergent thermodynamic structures [47,48], entanglement preparation [49–52], unconventional phase transitions [53–55], stochastic dynamics [56–62], and reservoir engineering in dissipative systems [63–69]. Our work addresses as yet unexplored questions on the propagation of correlations and that of information under measurement backaction. Our results indicate that, by harnessing backaction due to observation of individual quanta, correlations can propagate beyond the LR bound at the cost of the probabilistic nature of quantum measurement.

*Full-counting many-particle dynamics.*—We first illustrate our idea in a general way and then apply it to an exactly solvable model. Suppose that a quantum many-particle system is coupled to a Markovian reservoir and described by

 

$$\frac{d\hat{\rho}(t)}{dt} = -i(\hat{H}_{\rm eff}\hat{\rho} - \hat{\rho}\hat{H}_{\rm eff}^{\dagger}) + \mathcal{J}[\hat{\rho}], \tag{1}$$

where $\hat{\rho}(t)$ is the density matrix, $\hat{H}_{\rm eff} = \hat{H} - (i/2)\sum_a \hat{L}_a^{\dagger}\hat{L}_a$ is an effective non-Hermitian Hamiltonian with $\hat{L}_a$'s being Lindblad operators, and $\mathcal{J}[\hat{\rho}] = \sum_a \hat{L}_a\hat{\rho}\hat{L}_a^{\dagger}$ describes quantum jump processes [45,70–73]. Here and henceforth, we set $\hbar = 1$. Given an observed number $n$ of quantum jumps, we consider the full-counting many-particle dynamics described by the density matrix

$$\hat{\rho}^{(n)}(t) = \frac{\hat{\mathcal{P}}_n\hat{\rho}(t)\hat{\mathcal{P}}_n}{P_n(t)}, \tag{2}$$

where $\hat{\mathcal{P}}_n$ is a projector onto the subspace corresponding to $n$ jumps and $P_n(t) = \mathrm{Tr}[\hat{\mathcal{P}}_n\hat{\rho}(t)\hat{\mathcal{P}}_n]$ gives the probability of finding $n$ jumps during the time interval $[0, t]$. In this Letter, the jump process is assumed to be destructive; i.e., $\hat{L}_a$ causes the loss of a single particle. In practice, one can obtain $\hat{\rho}^{(n)}(t)$ by initially preparing $N$ particles, letting the system evolve during time $t$, and performing a global measurement to count the total number of particles. Note that a time record of quantum jumps must not be known here. In experiments, similar postselective operations have found important applications in ultracold atoms [26,30,74,75] and linear optics [76].

Decomposing the density matrix into the sum $\hat{\rho} = \sum_{n=0}^{N}\hat{\varrho}^{(n)}$ of unnormalized conditional density matrices $\hat{\varrho}^{(n)} = \hat{\mathcal{P}}_n\hat{\rho}\hat{\mathcal{P}}_n$, the time evolution can formally be solved as

$$\hat{\varrho}^{(n)}(t) = \sum_{\{a_k\}_{k=1}^{n}} \int_0^t dt_n \cdots \int_0^{t_2} dt_1 \prod_{k=1}^{n}\left[\hat{\mathcal{U}}_{\rm eff}(\Delta t_k)\hat{L}_{a_k}\right] \times \hat{\mathcal{U}}_{\rm eff}(t_1)\hat{\rho}(0)\hat{\mathcal{U}}_{\rm eff}^{\dagger}(t_1)\prod_{k=1}^{n}\left[\hat{L}_{a_k}^{\dagger}\hat{\mathcal{U}}_{\rm eff}^{\dagger}(\Delta t_k)\right], \tag{3}$$

where $\Delta t_k = t_{k+1} - t_k$ with $t_{n+1} \equiv t$, and $\hat{\mathcal{U}}_{\rm eff}(t) = e^{-i\hat{H}_{\rm eff}t}$. The solution (3) represents the ensemble average over all possible occurrences of $n$ quantum jump events.

As in closed systems [77–85], for unconditional open dynamics $\hat{\rho}(t) = \sum_n P_n(t)\hat{\rho}^{(n)}(t)$, the speed at which correlations build up between distant particles is known to be bounded by the LR velocity [45,86,87], provided that the Liouvillian in Eq. (1) consists of local operators. In contrast, for the full-counting dynamics $\hat{\rho}^{(n)}(t)$, the propagation speed is no longer expected to obey the LR velocity due to the nonlocal nature of the measurement that acts on an entire many-particle system. Here, we explore such hitherto unexplored nonequilibrium dynamics.

To be concrete, we focus on a simple exactly solvable model. Consider spin-polarized $N$ fermionic atoms trapped in a superlattice with the Hamiltonian $\hat{H} = -\sum_{l=0}^{L-1}[J(\hat{c}_{l+1}^{\dagger}\hat{c}_l + \hat{c}_l^{\dagger}\hat{c}_{l+1}) + (-1)^l h\hat{c}_l^{\dagger}\hat{c}_l]$. Here, $\hat{c}_l$ ($\hat{c}_l^{\dagger}$) is the annihilation (creation) operator of a spinless fermion at site $l$, $J$ is the hopping amplitude, and $h$ describes the on-site staggered potential. We assume that $L$ is even and that the system is initially half-filled, i.e., $N = L/2$. The system is subject to periodic boundary conditions and spatially periodic dissipation, which can be induced by a weak resonant optical lattice [Fig. 1(a)]. The time evolution is then described by the master equation (1) with the jump process $\mathcal{J}[\hat{\rho}] = 2\gamma\sum_l[2\hat{c}_l\hat{\rho}\hat{c}_l^{\dagger} + (-1)^l(\hat{c}_l\hat{\rho}\hat{c}_{l+1}^{\dagger} + \hat{c}_{l+1}\hat{\rho}\hat{c}_l^{\dagger})]$ and the effective Hamiltonian $\hat{H}_{\rm eff} = \hat{H}_{PT} - 2i\gamma\hat{N}$. Both of them consist of local operators and the resulting non-Hermitian Hamiltonian,

$$\begin{aligned}\hat{H}_{PT} &= -\sum_{l=0}^{L-1}[(J + (-1)^l i\gamma)(\hat{c}_{l+1}^{\dagger}\hat{c}_l + \hat{c}_l^{\dagger}\hat{c}_{l+1}) + (-1)^l h\hat{c}_l^{\dagger}\hat{c}_l] \\ &= \sum_{0\le k<2\pi}\sum_{\lambda=\pm}\epsilon_\lambda(k)\hat{g}_{\lambda k}^{\dagger}\hat{f}_{\lambda k},\end{aligned} \tag{4}$$

satisfies the $PT$ symmetry [46]; i.e., the symmetry with respect to the product of parity operation and time reversal. The jump part can be written in the diagonal form $\hat{L}_a = \sqrt{\gamma_{\lambda k}}\hat{d}_{\lambda k}$, with $\gamma_{\lambda k}$'s being positive coefficients and $\hat{d}_{\lambda k}$ being a linear combination of $\hat{c}_l$ [45]. Physically, this jump operator annihilates a single-particle mode with wave vector $k$.

In the last line of Eq. (4), the effective Hamiltonian $\hat{H}_{PT}$ is diagonalized with eigenvalues $\epsilon_{\pm}(k) = \pm\sqrt{h^2 - 4\gamma^2 + 2J'^2(1 + \cos(k))}$, where $J' = \sqrt{J^2 + \gamma^2}$ and $k = 2\pi n/(L/2)$ ($n = 0, 1, \ldots, L/2 - 1$). The operators $\hat{g}^{\dagger}$ and $\hat{f}$ create the right and left eigenvectors, i.e.,

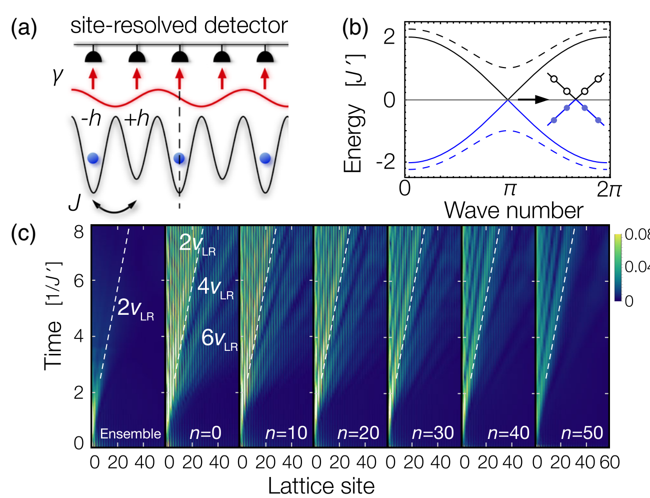


FIG. 1. (a) Fermions trapped in a superlattice and subject to a spatially modulated dissipative lattice (red), which causes atomic loss and breaks the parity symmetry with respect to the dashed line. The total atom number is measured by a site-resolved detector. (b) The top (black) and bottom (blue) bands of the effective Hamiltonian (4) for $\gamma = 0$, $h = J$ (dashed curves), and $\gamma/h = 1/2$ (solid curves). (c) Unconditional (left-most panel) and full-counting (other panels) equal-time correlations for different numbers $n$ of quantum jumps with $N = L/2 = 61$ and $\gamma = h/2 = 0.5J$. White dashed lines represent the light cone associated with the Lieb-Robinson bound.

$\hat{H}_{PT}\hat{g}^{\dagger}_{\lambda k}|0\rangle = \epsilon_{\lambda}(k)\hat{g}^{\dagger}_{\lambda k}|0\rangle$ and $\langle 0|\hat{f}_{\lambda k}\hat{H}_{PT} = \langle 0|\hat{f}_{\lambda k}\epsilon_{\lambda}(k)$, and they obey a generalized anticommutation relation $\{\hat{f}_{\lambda k}, \hat{g}^{\dagger}_{\lambda' k'}\} = \delta_{k,k'}\delta_{\lambda,\lambda'}$. A direct consequence of the non-Hermiticity is the nonorthogonality of eigenvectors. Specifically, $\hat{g}$ and $\hat{g}^{\dagger}$ satisfy an unusual anticommutation relation $\{\hat{g}_{\lambda k}, \hat{g}^{\dagger}_{\lambda' k'}\} = \delta_{k,k'}\Delta_{\lambda\lambda'}(k)$, where $\Delta_{\lambda\lambda'}(k)$ is the $\lambda\lambda'$ component of the $2 \times 2$ matrix whose nonzero off-diagonal elements indicate the nonorthogonality between the right eigenvectors of different bands in mode $k$.

When $\gamma < h/2$, $\hat{H}_{PT}$ has an entirely real, gapped band spectrum [dashed curves in Fig. 1(b)]. At $\gamma = h/2$, the band gap closes at $k = \pi$ [solid curves in Fig. 1(b)], and the $k = \pi$ eigenstates of the two bands coalesce into a single one. Such a point is known as an exceptional point [88] or, in the thermodynamic limit, as the spectral singularity [89]. Above the threshold $\gamma > h/2$, some eigenmodes around $k = \pi$ turn out to have complex pairs of pure imaginary eigenvalues. For simplicity, we assume that $L/2$ is odd such that the singularity at $k = \pi$ is avoided [see the inset in Fig. 1(b)] [90].

*Nonlocal propagation of correlations.*—Combining a general solution (3) and the diagonalized effective Hamiltonian (4), we obtain an exact solution of the full-counting dynamics $\hat{\rho}^{(n)}(t)$ [45]. By way of illustration, we consider the following quench dynamics. Initially, the staggered potential $h$ and the dissipation $\gamma$ are switched off and the system is prepared in the ground state of $\hat{H}$. We then suddenly switch on $h$ and $\gamma$, and we let the system evolve according to Eq. (1). We choose $\gamma = h/2$, such that the parameters of the postquench Hamiltonian $\hat{H}_{PT}$ are set to the real-to-complex spectrum transition point, leading to the linear dispersion around $k = \pi$ [Fig. 1(b)].

Let us first discuss the unconditional case $\hat{\rho}(t) = \sum_{n=0}^{N} P_n(t)\hat{\rho}^{(n)}(t)$. The left-most panel in Fig. 1(c) plots an equal-time correlation $C(l,t) = \mathrm{Tr}[\hat{\rho}(t)\hat{c}^{\dagger}_{l}\hat{c}_0]$, which exhibits a blurred light cone [91]. Since the Liouvillian in Eq. (1) consists of local operators, it is expected that correlations can propagate no faster than twice the LR velocity $2v_{\mathrm{LR}}$ [28,45,86,87], where $v_{\mathrm{LR}}$ is given by the maximum group velocity $|\partial\epsilon_{\pm}(k)/\partial(k/2)|_{k=\pi} = 2J'$ [92].

The situation is quite different in the full-counting dynamics $\hat{\rho}^{(n)}(t)$ in Eq. (2). Figure 1(c) plots an equal-time correlation $C^{(n)}(l,t) = \mathrm{Tr}[\hat{\rho}^{(n)}(t)\hat{c}^{\dagger}_{l}\hat{c}_0]$ for such dynamics with different values of $n$. We find nonlocal modes that propagate faster than the LR velocity of the corresponding unconditional dynamics. Moreover, velocities of such supersonic modes appear at integer multiples of $2v_{\mathrm{LR}}$. Physically, the propagations beyond the LR bound signals nonlocality encoded in the full-counting dynamics $\hat{\rho}^{(n)}(t)$.

The origin of these nonlocal propagations can be understood from the underlying dynamics governed by the effective non-Hermitian Hamiltonian $\hat{H}_{PT}$, which describes time evolution during an interval without quantum jumps [45]. To clarify the essential point, let us focus on a simple quantum trajectory containing null jumps: $\hat{\rho}^{(0)}(t) = e^{-i\hat{H}_{PT}t}\hat{\rho}(0)e^{i\hat{H}^{\dagger}_{PT}t}/\mathrm{Tr}[e^{-i\hat{H}_{PT}t}\hat{\rho}(0)e^{i\hat{H}^{\dagger}_{PT}t}]$, where the factor $-2i\gamma\hat{N}$ in $\hat{H}_{\mathrm{eff}}$ cancels out in forming the ratio. A similar time evolution has been discussed in dissipative evolutions [93] and $PT$-symmetric quantum systems [94,95]. An initially pure state remains pure in these dynamics [94]. Denoting $\hat{\rho}(0) = |\Psi_0\rangle\langle\Psi_0|$, we introduce an unnormalized time-dependent wave function $|\Psi_t\rangle = e^{-i\hat{H}_{PT}t}|\Psi_0\rangle$. We first expand the initial state $|\Psi_0\rangle$ in terms of right eigenvectors: $|\Psi_0\rangle = \prod_k[\sum_{\lambda}\psi_{\lambda k}\hat{g}^{\dagger}_{\lambda k}]|0\rangle$, where $\psi_{\lambda k}$'s are expansion coefficients. We then introduce the unequal-time correlation by $\tilde{C}^{(0)}(l,t) = \langle\Psi_0|\hat{c}^{\dagger}_{l}(t)\hat{c}_0(0)|\Psi_0\rangle/\langle\Psi_t|\Psi_t\rangle$ with $\hat{c}^{\dagger}_{l}(t) = e^{i\hat{H}^{\dagger}_{PT}t}\hat{c}^{\dagger}_{l}e^{-i\hat{H}_{PT}t}$, which can be calculated as

$$\tilde{C}^{(0)}(l,t) = \frac{2}{L}\sum_{k}\sum_{\lambda=\pm}\left\{\begin{matrix}\alpha_{\lambda k}\\ \beta_{\lambda k}\end{matrix}\right\}\frac{\psi^{*}_{\lambda k}e^{i\epsilon_{\lambda}(k)t - ik\lceil l/2\rceil}}{\mathcal{N}_k(t)}. \quad (5)$$

Here, $\alpha_{\lambda k}$ and $\beta_{\lambda k}$ are coefficients chosen according to the parity of $l$ [45], $\lceil\cdot\rceil$ is the ceiling function, and $\mathcal{N}_k(t) = \sum_{\lambda\lambda'=\pm}\psi^{*}_{\lambda k}(t)\Delta_{\lambda\lambda'}(k)\psi_{\lambda' k}(t)$, where $\psi_{\lambda k}(t) = \psi_{\lambda k}e^{-i\epsilon_{\lambda}(k)t}$. The total norm of an unnormalized quantum state $|\Psi_t\rangle$ is then given by $\langle\Psi_t|\Psi_t\rangle = \prod_k\mathcal{N}_k(t)$.

A crucial observation here is that due to the nonorthogonality of eigenvectors ($\Delta_{+-} = \Delta^{*}_{-+} \neq 0$), the norm $\mathcal{N}_k(t)$ oscillates at frequency $2\epsilon_{+}(k)$. Thus, $\tilde{C}^{(0)}(l,t)$ in Eq. (5) involves terms that oscillate at frequencies $\epsilon_{\lambda}(k), 3\epsilon_{\lambda}(k), 5\epsilon_{\lambda}(k), \ldots$, leading to the propagations at velocities $v_{\mathrm{LR}}, 3v_{\mathrm{LR}}, 5v_{\mathrm{LR}}, \ldots$ [Fig. 2(a)]. In contrast, the equal-time correlation $C^{(0)}(l,t)$ involves the propagations at velocities $2v_{\mathrm{LR}}, 4v_{\mathrm{LR}}, 6v_{\mathrm{LR}}, \ldots$ [Fig. 2(b)], as it is formed by quasiparticle pairs propagating with velocities $v_{\mathrm{LR}}, 3v_{\mathrm{LR}}, 5v_{\mathrm{LR}}, \ldots$ [77] [Fig. 2(c)].

The emergence of these supersonic modes is a consequence of the interplay between non-Hermiticity and the many-particle nature of the system. The appearance

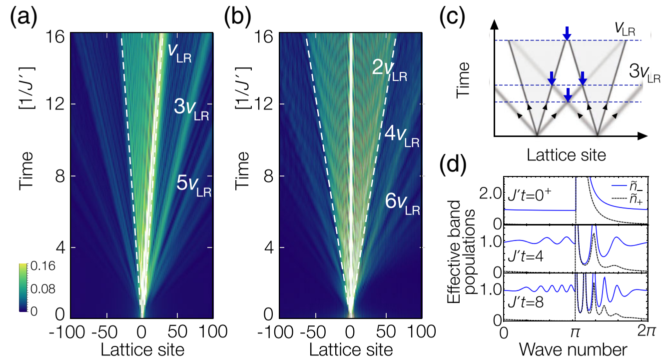


FIG. 2. (a) Unequal- and (b) equal-time correlations plotted for $N = L/2 = 61$ and $\gamma = h/2 = 0.5J$. The white dashed lines indicate the Lieb-Robinson bound. (c) An illustration of how the correlation is carried by quasiparticles propagating at velocities $v_{\mathrm{LR}}$ and $3v_{\mathrm{LR}}$. (d) The effective band populations for different times $J't = 0^{+}$ (postquench state), 4, and 8.

of the oscillating norm factors $\mathcal{N}_k(t)$ in the denominator in Eq. (5) originates from the fact that the total norm of a many-particle quantum state is given by their product. Thus, the supersonic modes have no counterparts in the single-particle sector or the mean-field non-Hermitian dynamics in optics [96,97] and dissipative matter waves [39,98–100], where the total norm is determined by the sum rather than the product of $\mathcal{N}_k(t)$ [101].

In analogy with closed systems [77–85], we may regard $\tilde{n}_{\lambda k}(t) = |\psi_{\lambda k}|^2/\mathcal{N}_k(t)$ as an effective band population of quasiparticles. In noninteracting closed systems, the band population remains constant after the quench [77,83–85]. In contrast, the effective band population oscillates in time [Fig. 2(d)] due to the nonorthogonality between two eigenvectors in a mode $k$. Since the interference for the same momentum implies a nonlocal coupling in real space, we may interpret the supersonic propagation as a consequence of such a nonlocal, self-interaction of quasiparticles.

*Chirality in propagation of correlations.*—Yet another feature of the observed propagation is its chirality. Here, by chirality we mean that the violation of the left-right symmetry of propagation of correlations. This symmetry breaking results from the parity violation in the effective Hamiltonian; i.e., $\hat{H}_{PT}$ is not invariant under $l \to -l$ [Fig. 1(a)]. We can intuitively interpret the pronounced propagation in the right direction as found in Figs. 2(a) and 2(b), on the basis of the gain-loss structure of $\hat{H}_{PT}$. Imagine that particles are injected at the "gain" bond having positive imaginary hopping $+i\gamma$ [inset of Fig. 3(a)]. Then, a majority of the particles flow into the deeper, right potential. The injected particles are removed at the "loss" bond, and thus, local flows of particles can be formed. Overall, the flow in the right direction outweighs the reverse flow, resulting in a net positive current.

A nontrivial feature here is that the chirality is most pronounced at the spectrum transition point of $\hat{H}_{PT}$. Figure 3(a) shows the current $iJ\sum_{l=0}^{L-1}(\hat{c}_l^\dagger \hat{c}_{l+1} - \hat{c}_{l+1}^\dagger \hat{c}_l)$ in a long-time regime for different values of $h$ and $\gamma$. The pronounced chirality at the threshold $\gamma = h/2$ originates from the emergence of the exceptional point at $k = \pi$ [Fig. 1(b)] [102]. In its vicinity, the strong nonorthogonality induces coalescence of two eigenvectors of different bands into the one associated with the band dispersion having positive group velocities $\partial\epsilon/\partial(k/2) > 0$ [45]. This confluent band structure leads to imbalanced effective band populations $\tilde{n}_{\lambda k}(t)$ in Fig. 2(d), where the population $\tilde{n}_{+,k}$ of the upper band almost vanishes for $k < \pi$, while $\tilde{n}_{-,k}$ takes a value close to unity. Such an effective violation of the particle-hole symmetry generates quasiparticles having positive group velocities [cf. Fig. 1(b)], leading to the pronounced propagation of correlations in the right direction.

It is noteworthy that, in contrast to the single-particle sector [103–108], the chirality in the present case is prominent owing to the formation of the Fermi sea at $\epsilon_F = 0$; low-energy excitations are subject to the strong nonorthogonality

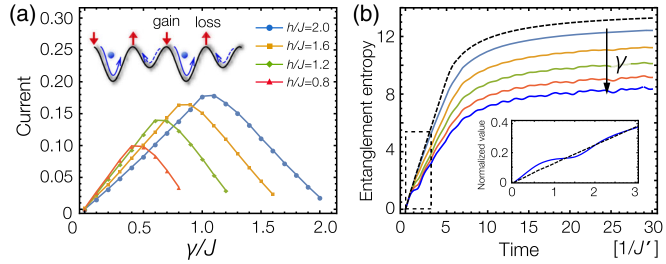


FIG. 3. (a) The current averaged over the time interval between $t = 15/J'$ and $20/J'$ plotted against the strength of dissipation $\gamma$ for different on site potentials $h$. The inset shows a gain-loss situation for a positive particle current. (b) The time evolutions of entanglement entropy of a chain of length 20, starting from a product state (the ground state of $\hat{H}$ with $h = \infty$). We vary a postquench parameter $\gamma$ from 0.0 to 0.5 (top to bottom) with step 0.1 and $\gamma = h/2$ held fixed. The inset magnifies the short-time regime showing the oscillatory behavior due to the time-dependent effective band populations.

that becomes maximal at the gap closing point $k = \pi$. The resulting unidirectionality appears as the chiral propagation of correlations in the case of many-particle systems.

The chirality also has a physical consequence in the entanglement growth of the system. Figure 3(b) shows the time evolution of the entanglement entropy $S_A[\hat{\rho}^{(0)}(t)]$ [109] after the quench for different values of $\gamma$ with subregion $A$ of a chain of 20 sites. A decrease in the entanglement entropy with increasing $\gamma$ can be interpreted as a consequence of the chirality. The quantum quench generates pairs of entangled quasiparticles propagating in opposite directions [77]. The entanglement entropy essentially measures the number of quantum-mechanically correlated pairs, such that one quasiparticle is inside and the other is outside of subregion $A$. Since the chiral (unidirectional) modes do not generate such entangled pairs moving in opposite directions, the chirality leads to a decrease in the entanglement entropy.

An oscillation on top of a linear increase in the entanglement entropy [inset in Fig. 3(b)] results from the time-dependent effective band populations $\tilde{n}_{\lambda k}(t)$. In view of the simple dispersion of the present model, this presents yet another unique feature of open quantum dynamics because, in closed integrable systems, such oscillations of entanglement entropy emerge only if there exist multiple local maxima in a band dispersion [83].

*Discussions.*—As a possible experimental test of the present consideration, we propose to using site-resolved measurements [14–23] to probe the full-counting dynamics. The dissipation can be implemented by superimposing a weak resonant optical lattice [40–42,98,110,111] [see Fig. 1(a)]. The parameters $\gamma$, $J$, $h$ are experimentally tuned by controlling the intensities of optical beams. Using fermionic quantum gas microscopy [17–21], one can measure the site-resolved density-density correlation and the total number of particles simultaneously. Since the connected density-density correlation in noninteracting models reduces to the product of the equal-time correlations, both correlations share the same information. While detecting supersonic propagations will be challenging at long times, they should be observable in a short-time regime such that a relatively large number of atoms still remain in the trap. For example, if one chooses $\gamma = h/2 = 0.25J$ and $N = 61$, the probability of detecting trajectories with lost particles less than the half of the initial total particle number can exceed $\sim 20\%$ up to $tJ' \lesssim 3$ at which supersonic propagations, similar to the ones in Fig. 1(c), are visible. In practice, one may choose $^6$Li atoms and use an optical beam resonant with the $^2S_{1/2} \to {}^2P_{3/2}$ transition, as recently demonstrated in Ref. [42].

The ability of measuring individual quanta can reveal the emergence of unique many-particle dynamics that cannot be seen in closed systems. Our results show that correlations can propagate faster than the LR bound at the cost of the probabilistic nature of quantum measurement. The emergence of the nonlocal propagation originates from the nonorthogonality of eigenvectors due to the non-Hermiticity of the underlying dynamics. In view of the generality of nonorthogonality in non-Hermitian systems, the nonlocal propagation can also appear in a variety of other open many-particle systems. Such features will become most prominent when nonorthogonality becomes maximal due to, for example, the presence of an exceptional point as demonstrated in our Letter. It is intriguing to explore the roles of interactions [79,80] or nonintegrablility [81,82] in such unconventional many-body dynamics subject to single-quantum-resolved measurement. Analogous to closed systems [77,78], it is of interest to develop field-theoretic arguments. It is noteworthy that the low-energy field theory [112] of the effective Hamiltonian $\hat{H}_{PT}$ corresponds to the quantum Liouville theory, which attracts much attention in high-energy physics [113]. We hope that the present work stimulates further studies in these directions.

We are grateful to Juan P. Garrahan, Peter Rabl, Vladimir Konotop, Yogesh Joglekar, Naomichi Hatano, Jörg Schmiedmayer, Shunsuke Furukawa, Hosho Katsura, Takashi Mori, Keiji Saito, and Zala Lenarcic for valuable discussions. We acknowledge support from KAKENHI Grant No. JP26287088 from the Japan Society for the Promotion of Science (JSPS), and a Grant-in-Aid for Scientific Research on Innovative Areas "Topological Materials Science" (KAKENHI Grant No. JP15H05855), and the Photon Frontier Network Program from MEXT of Japan, ImPACT Program of Council for Science, Technology and Innovation (Cabinet Office, Government of Japan). Y. A. acknowledges support from JSPS (Grant No. JP16J03613).

[1] W. Lu, Z. Ji, L. Pfeiffer, K. W. West, and A. J. Rimberg, Nature (London) **423**, 422 (2003).

[2] T. Fujisawa, T. Hayashi, Y. Hirayama, H. D. Cheong, and Y. H. Jeong, Appl. Phys. Lett. **84**, 2343 (2004).

[3] J. Bylander, T. Duty, and P. Delsing, Nature (London) **434**, 361 (2005).

[4] S. Gustavsson, R. Leturcq, B. Simovič, R. Schleser, T. Ihn, P. Studerus, K. Ensslin, D. C. Driscoll, and A. C. Gossard, Phys. Rev. Lett. **96**, 076605 (2006).

[5] M. D. Eisaman, J. Fan, A. Migdall, and S. V. Polyakov, Rev. Sci. Instrum. **82**, 071101 (2011).

[6] L. S. Levitov, H. Lee, and G. B. Lesovik, J. Math. Phys. (N.Y.) **37**, 4845 (1996).

[7] W. Belzig and Y. V. Nazarov, Phys. Rev. Lett. **87**, 197006 (2001).

[8] K. Saito and Y. Utsumi, Phys. Rev. B **78**, 115429 (2008).

[9] M. Esposito, U. Harbola, and S. Mukamel, Rev. Mod. Phys. **81**, 1665 (2009).

[10] E. Altman, E. Demler, and M. D. Lukin, Phys. Rev. A **70**, 013603 (2004).

[11] A. Polkovnikov, E. Altman, and E. Demler, Proc. Natl. Acad. Sci. U.S.A. **103**, 6125 (2006).

[12] S. Hofferberth, I. Lesanovsky, T. Schumm, A. Imambekov, V. Gritsev, E. Demler, and J. Schmiedmayer, Nat. Phys. **4**, 489 (2008).

[13] I. Klich and L. Levitov, Phys. Rev. Lett. **102**, 100502 (2009).

[14] W. S. Bakr, J. I. Gillen, A. Peng, S. Fölling, and M. Greiner, Nature (London) **462**, 74 (2009).

[15] J. F. Sherson, C. Weitenberg, M. Endres, M. Cheneau, I. Bloch, and S. Kuhr, Nature (London) **467**, 68 (2010).

[16] M. Miranda, R. Inoue, Y. Okuyama, A. Nakamoto, and M. Kozuma, Phys. Rev. A **91**, 063414 (2015).

[17] L. W. Cheuk, M. A. Nichols, M. Okan, T. Gersdorf, V. V. Ramasesh, W. S. Bakr, T. Lompe, and M. W. Zwierlein, Phys. Rev. Lett. **114**, 193001 (2015).

[18] M. F. Parsons, F. Huber, A. Mazurenko, C. S. Chiu, W. Setiawan, K. Wooley-Brown, S. Blatt, and M. Greiner, Phys. Rev. Lett. **114**, 213002 (2015).

[19] E. Haller, J. Hudson, A. Kelly, D. A. Cotta, P. Bruno, G. D. Bruce, and S. Kuhr, Nat. Phys. **11**, 738 (2015).

[20] A. Omran, M. Boll, T. A. Hilker, K. Kleinlein, G. Salomon, I. Bloch, and C. Gross, Phys. Rev. Lett. **115**, 263001 (2015).

[21] G. J. A. Edge, R. Anderson, D. Jervis, D. C. McKay, R. Day, S. Trotzky, and J. H. Thywissen, Phys. Rev. A **92**, 063406 (2015).

[22] R. Yamamoto, J. Kobayashi, T. Kuno, K. Kato, and Y. Takahashi, New J. Phys. **18**, 023016 (2016).

[23] A. Alberti, C. Robens, W. Alt, S. Brakhane, M. Karski, R. Reimann, A. Widera, and D. Meschede, New J. Phys. **18**, 053010 (2016).

[24] M. Cheneau, P. Barmettler, D. Poletti, M. Endres, P. Schauss, T. Fukuhara, C. Gross, I. Bloch, C. Kollath, and S. Kuhr, Nature (London) **481**, 484 (2012).

[25] T. Langen, R. Geiger, M. Kuhnert, B. Rauer, and J. Schmiedmayer, Nat. Phys. **9**, 640 (2013).

[26] T. Fukuhara, S. Hild, J. Zeiher, P. Schauß, I. Bloch, M. Endres, and C. Gross, Phys. Rev. Lett. **115**, 035302 (2015).

[27] E. H. Lieb and D. W. Robinson, Commun. Math. Phys. **28**, 251 (1972).

[28] S. Bravyi, M. B. Hastings, and F. Verstraete, Phys. Rev. Lett. **97**, 050401 (2006).

[29] B. Nachtergaele, Y. Ogata, and R. Sims, J. Stat. Phys. **124**, 1 (2006).
[30] R. Islam, R. Ma, P. M. Preiss, M. E. Tai, A. Lukin, M. Rispoli, and M. Greiner, Nature (London) **528**, 77 (2015).
[31] M. F. Parsons, A. Mazurenko, C. S. Chiu, G. Ji, D. Greif, and M. Greiner, Science **353**, 1253 (2016).
[32] M. Boll, T. A. Hilker, G. Salomon, A. Omran, J. Nespolo, L. Pollet, I. Bloch, and C. Gross, Science **353**, 1257 (2016).
[33] L. W. Cheuk, M. A. Nichols, K. R. Lawrence, M. Okan, H. Zhang, E. Khatami, N. Trivedi, T. Paiva, M. Rigol, and M. W. Zwierlein, Science **353**, 1260 (2016).
[34] A. Mazurenko, C. S. Chiu, G. Ji, M. F. Parsons, M. Kanász-Nagy, R. Schmidt, F. Grusdt, E. Demler, D. Greif, and M. Greiner, Nature (London) **545**, 462 (2017).
[35] P. Jurcevic, B. P. Lanyon, P. Hauke, C. Hempel, P. Zoller, R. Blatt, and C. F. Roos, Nature (London) **511**, 202 (2014).
[36] P. Richerme, Z.-X. Gong, A. Lee, C. Senko, J. Smith, M. Moss-Feig, S. Michalakis, A. V. Gorshkov, and C. Monroe, Nature (London) **511**, 198 (2014).
[37] D. Poletti, J.-S. Bernier, A. Georges, and C. Kollath, Phys. Rev. Lett. **109**, 045302 (2012).
[38] D. Poletti, P. Barmettler, A. Georges, and C. Kollath, Phys. Rev. Lett. **111**, 195301 (2013).
[39] G. Barontini, R. Labouvie, F. Stubenrauch, A. Vogler, V. Guarrera, and H. Ott, Phys. Rev. Lett. **110**, 035302 (2013).
[40] B. Rauer, P. Grišins, I. E. Mazets, T. Schweigler, W. Rohringer, R. Geiger, T. Langen, and J. Schmiedmayer, Phys. Rev. Lett. **116**, 030402 (2016).
[41] H. P. Lüschen, P. Bordia, S. S. Hodgman, M. Schreiber, S. Sarkar, A. J. Daley, M. H. Fischer, E. Altman, I. Bloch, and U. Schneider, Phys. Rev. X **7**, 011034 (2017).
[42] J. Li, A. K. Harter, J. Liu, L. de Melo, Y. N. Joglekar, and L. Luo, arXiv:1608.05061.
[43] Y. S. Patil, S. Chakram, and M. Vengalattore, Phys. Rev. Lett. **115**, 140402 (2015).
[44] T. Tomita, S. Nakajima, I. Danshita, Y. Takasu, and Y. Takahashi, Sci. Adv. **3**, e1701513 (2017).
[45] See Supplemental Material at http://link.aps.org/supplemental/10.1103/PhysRevLett.120.185301 for the background of quantum trajectory method and the Lieb-Robinson bound and also for technical details about derivations of the results.
[46] C. M. Bender and S. Boettcher, Phys. Rev. Lett. **80**, 5243 (1998).
[47] J. P. Garrahan and I. Lesanovsky, Phys. Rev. Lett. **104**, 160601 (2010).
[48] C. Flindt and J. P. Garrahan, Phys. Rev. Lett. **110**, 050601 (2013).
[49] T. E. Lee, F. Reiter, and N. Moiseyev, Phys. Rev. Lett. **113**, 250401 (2014).
[50] M. K. Pedersen, J. J. W. H. Srensen, M. C. Tichy, and J. F. Sherson, New J. Phys. **16**, 113038 (2014).
[51] A. C. J. Wade, J. F. Sherson, and K. Mølmer, Phys. Rev. Lett. **115**, 060401 (2015).
[52] T. J. Elliott, W. Kozlowski, S. F. Caballero-Benitez, and I. B. Mekhov, Phys. Rev. Lett. **114**, 113604 (2015).
[53] T. E. Lee and C.-K. Chan, Phys. Rev. X **4**, 041001 (2014).
[54] S. Dhar and S. Dasgupta, Phys. Rev. A **93**, 050103 (2016).
[55] Y. Ashida, S. Furukawa, and M. Ueda, Phys. Rev. A **94**, 053615 (2016).
[56] M. D. Lee and J. Ruostekoski, Phys. Rev. A **90**, 023628 (2014).
[57] S. Dhar, S. Dasgupta, A. Dhar, and D. Sen, Phys. Rev. A **91**, 062115 (2015).
[58] Y. Ashida and M. Ueda, Phys. Rev. Lett. **115**, 095301 (2015).
[59] T. J. Elliott and V. Vedral, Phys. Rev. A **94**, 012118 (2016).
[60] W. Kozlowski, S. F. Caballero-Benitez, and I. B. Mekhov, Sci. Rep. **7**, 42597 (2017).
[61] Y. Ashida and M. Ueda, Phys. Rev. A **95**, 022124 (2017).
[62] S. Lahiri and A. Dhar, arXiv:1708.06496.
[63] A. Beige, D. Braun, B. Tregenna, and P. L. Knight, Phys. Rev. Lett. **85**, 1762 (2000).
[64] F. Verstraete, M. M. Wolf, and J. I. Cirac, Nat. Phys. **5**, 633 (2009).
[65] W. Yi, S. Diehl, A. J. Daley, and P. Zoller, New J. Phys. **14**, 055002 (2012).
[66] P. Hauke, R. J. Sewell, M. W. Mitchell, and M. Lewenstein, Phys. Rev. A **87**, 021601 (2013).
[67] K. Stannigel, P. Hauke, D. Marcos, M. Hafezi, S. Diehl, M. Dalmonte, and P. Zoller, Phys. Rev. Lett. **112**, 120406 (2014).
[68] T. J. Elliott and I. B. Mekhov, Phys. Rev. A **94**, 013614 (2016).
[69] C. Joshi, J. Larson, and T. P. Spiller, Phys. Rev. A **93**, 043818 (2016).
[70] R. Dum, P. Zoller, and H. Ritsch, Phys. Rev. A **45**, 4879 (1992).
[71] J. Dalibard, Y. Castin, and K. Mølmer, Phys. Rev. Lett. **68**, 580 (1992).
[72] H. Carmichael, *An Open System Approach to Quantum Optics* (Springer, Berlin, 1993).
[73] A. J. Daley, Adv. Phys. **63**, 77 (2014).
[74] M. Endres, M. Cheneau, T. Fukuhara, C. Weitenberg, P. Schauß, C. Gross, L. Mazza, M. C. Bañuls, L. Pollet, I. Bloch, and S. Kuhr, Science **334**, 200 (2011).
[75] I. Bloch, J. Dalibard, and W. Zwerger, Rev. Mod. Phys. **80**, 885 (2008).
[76] P. Kok, W. J. Munro, K. Nemoto, T. C. Ralph, J. P. Dowling, and G. J. Milburn, Rev. Mod. Phys. **79**, 135 (2007).
[77] P. Calabrese and J. Cardy, J. Stat. Mech. (2005) P04010.
[78] P. Calabrese and J. Cardy, Phys. Rev. Lett. **96**, 136801 (2006).
[79] C. Kollath, A. M. Läuchli, and E. Altman, Phys. Rev. Lett. **98**, 180601 (2007).
[80] M. Collura, P. Calabrese, and F. H. L. Essler, Phys. Rev. B **92**, 125131 (2015).
[81] H. Kim and D. A. Huse, Phys. Rev. Lett. **111**, 127205 (2013).
[82] M. Kormos, M. Collura, G. Takács, and P. Calabrese, Nat. Phys. **13**, 246 (2017).
[83] M. Fagotti and P. Calabrese, Phys. Rev. A **78**, 010306 (2008).
[84] V. Eisler and I. Peschel, Ann. Phys. (Amsterdam) **17**, 410 (2008).
[85] R. Geiger, T. Langen, I. E. Mazets, and J. Schmiedmayer, New J. Phys. **16**, 053034 (2014).

[86] D. Poulin, Phys. Rev. Lett. **104**, 190401 (2010).
[87] M. Kliesch, C. Gogolin, and J. Eisert, in *Many-Electron Approaches in Physics, Chemistry and Mathematics* (Springer, Cham, 2014), pp. 301–318.
[88] T. Kato, *Perturbation Theory for Linear Operators* (Springer, New York, 1966).
[89] A. Mostafazadeh, Phys. Rev. Lett. **102**, 220402 (2009).
[90] For an even $L/2$, one can impose the anti-periodic boundary conditions to ensure that $k = \pi$ is avoided.
[91] J.-S. Bernier, R. Tan, L. Bonnes, C. Guo, D. Poletti, and C. Kollath, Phys. Rev. Lett. **120**, 020401 (2018).
[92] Here a factor of two in the group velocity comes from our choice of wave vectors defined in the Fourier transformations of the sublattices [see Eq. (5)].
[93] N. Gisin, J. Phys. A **14**, 2259 (1981).
[94] D. C. Brody and E.-M. Graefe, Phys. Rev. Lett. **109**, 230405 (2012).
[95] K. Kawabata, Y. Ashida, and M. Ueda, Phys. Rev. Lett. **119**, 190401 (2017).
[96] C. E. Ruter, K. G. Makris, R. El-Ganainy, D. N. Christodoulides, M. Segev, and D. Kip, Nat. Phys. **6**, 192 (2010).
[97] A. Regensburger, C. Bersch, M.-A. Miri, G. Onishchukov, D. N. Christodoulides, and U. Peschel, Nature (London) **488**, 167 (2012).
[98] P. Peng, W. Cao, C. Shen, W. Qu, W. Jianming, L. Jiang, and Y. Xiao, Nat. Phys. **12**, 1139 (2016).
[99] T. Gao, E. Estrecho, K. Y. Bliokh, T. C. H. Liew, M. D. Fraser, S. Brodbeck, M. Kamp, C. Schneider, S. Hofling, Y. Yamamoto, F. Nori, Y. S. Kivshar, A. G. Truscott, R. G. Dall, and E. A. Ostrovskaya, Nature (London) **526**, 554 (2015).
[100] V. V. Konotop, J. Yang, and D. A. Zezyulin, Rev. Mod. Phys. **88**, 035002 (2016).
[101] K. G. Makris, R. El-Ganainy, D. N. Christodoulides, and Z. H. Musslimani, Phys. Rev. Lett. **100**, 103904 (2008).
[102] W. Heiss and H. Harney, Eur. Phys. J. D **17**, 149 (2001).
[103] S. Longhi, Phys. Rev. Lett. **103**, 123601 (2009).
[104] S. Longhi, Phys. Rev. A **81**, 022102 (2010).
[105] Z. Lin, H. Ramezani, T. Eichelkraut, T. Kottos, H. Cao, and D. N. Christodoulides, Phys. Rev. Lett. **106**, 213901 (2011).
[106] D. D. Scott and Y. N. Joglekar, Phys. Rev. A **85**, 062105 (2012).
[107] L. Feng, Y.-L. Xu, W. S. Fegadolli, M.-H. Lu, J. E. B. Oliveira, V. R. Almeida, Y.-F. Chen, and A. Scherer, Nat. Mater. **12**, 108 (2013).
[108] J. Wiersig, Phys. Rev. A **89**, 012119 (2014).
[109] I. Peschel, J. Phys. A **36**, L205 (2003).
[110] M. K. Oberthaler, R. Abfalterer, S. Bernet, C. Keller, J. Schmiedmayer, and A. Zeilinger, Phys. Rev. A **60**, 456 (1999).
[111] A. Turlapov, A. Tonyushkin, and T. Sleator, Phys. Rev. A **68**, 023408 (2003).
[112] Y. Ashida, S. Furukawa, and M. Ueda, Nat. Commun. **8**, 15791 (2017).
[113] N. Seiberg, *Notes on Quantum Liouville Theory and Quantum Gravity* (Springer US, Boston, 1991), pp. 363–395.